IEEE Access
Multidisciplinary | Rapid Review | Open Access Journal

Received January 29, 2019, accepted February 23, 2019, date of publication February 27, 2019, date of current version March 18, 2019.

Digital Object Identifier 10.1109/ACCESS.2019.2901939

Subcarrier and Power Allocations for Dimmable Enhanced ADO-OFDM With Iterative Interference Cancellation

XUAN HUANG[1], FANG YANG[1,2], (Senior Member, IEEE), XUAN LIU[3], HAILONG ZHANG[3], JUN YE[4], AND JIAN SONG[1,2], (Fellow, IEEE)

[1]Department of Electronic Engineering, Beijing National Research Center for Information Science and Technology, Tsinghua University, Beijing 100084, China
[2]Key Laboratory of Digital TV System of Guangdong Province and Shenzhen City, Research Institute of Tsinghua University in Shenzhen, Shenzhen 518057, China
[3]China Electric Power Research Institute, Beijing 100192, China
[4]State Grid Chongqing Electric Power Company Electric Power Research Institute, Chongqing 400123, China

Corresponding author: Fang Yang (fangyang@tsinghua.edu.cn)

This work was supported by the Science and Technology Project of State Grid Corporation of China (SGCC) under Grant JLB17201800070 (Research on the interoperability and coexistence technology of broadband power line communication for power consumption information collection).

ABSTRACT In this paper, a novel modulation scheme called enhanced asymmetrically clipped DC-biased optical OFDM (eADO-OFDM) is proposed to accommodate different demands of multi-users in downlink multiple access for visible light communication systems. Meanwhile, to satisfy various dimming levels, enhanced negative ADO-OFDM (eNADO-OFDM) is investigated and combined with eADO-OFDM for multiplexing transmission. By adjusting the proportion of these two signals, the dimming control scheme can be achieved, while the entire dynamic range of light-emitting diodes is exploited. In order to achieve superior transmission performance, the optimal power allocation under the desired dimming level is studied to minimize the overall bit error rate (BER). Moreover, to obtain more accurate estimation, an iterative receiver with interference cancellation, in which the pairwise averaging and pairwise clipping are exploited, is proposed. The simulation results show that the proposed scheme can effectively carry out the dimming control with wide dimming range for illumination and achieve superior BER performance at the same signal-to-noise ratio compared to the conventional counterparts, while only a few iterations are required.

INDEX TERMS Visible light communications (VLC), enhanced asymmetrically clipped DC biased optical OFDM (eADO-OFDM), interference cancellation, power allocation, dimming control.

I. INTRODUCTION

Owing to the advantages of supporting modulation and lighting at the same time [1], light-emitting diode (LED) has been gradually popularized in recent years, resulting in a lot of attention for visible light communication (VLC) systems, which are green, low-carbon, low-cost, and have broad license-free bandwidth [2]. Theoretically, in an optical wireless communication system, as long as there is light, the information transmission with high speed can be realized. VLC can effectively avoid the weaknesses of signal leakage, and quickly establish a safe information space for anti-jamming and anti-interception [3].

In recent years, orthogonal frequency division multiplexing (OFDM) has been widely applied in VLC systems due to its high spectral efficiency and the capability of resisting inter-symbol interference (ISI) [4]. Intensity modulation and direct detection (IM/DD) is usually adopted in the OFDM-based optical wireless communication systems [5]. For an OFDM-based system with IM/DD, the transmitted signal is modulated onto the intensity of light, which means the transmitted signal should be real and non-negative [6]. The real values can be ensured by imposing the Hermitian symmetry to the symbols in the frequency domain [7]. And the non-negative values can be realized by several different optical OFDM methods, such as direct current biased optical OFDM (DCO-OFDM) which is inefficient in optical power because of the DC bias [7], asymmetrically clipped optical OFDM (ACO-OFDM) which is inefficient in the aspect of spectral efficiency due to the non-utilization of even subcarriers [8], and pulse-amplitude-modulated discrete multitone (PAM-DMT) which is also inefficient in the terms of spectral

The associate editor coordinating the review of this manuscript and approving it for publication was Donatella Darsena.

efficiency since the lack of real part of the signal [9]. Based on the conventional schemes, several novel hybrid modulation schemes are further proposed. In [10], asymmetrically clipped DC biased optical OFDM (ADO-OFDM) is addressed, where the odd subcarriers and even subcarriers adopt ACO-OFDM and DCO-OFDM, respectively. Hybrid ACO-OFDM (HACO-OFDM) is investigated in [11], where the odd subcarriers utilize ACO-OFDM, and the even subcarriers apply PAM-DMT. Recently, a new technology called layered ACO-OFDM is proposed by combining different layers of ACO-OFDM signals [12].

However, the number of subcarriers allocated to one type of modulation scheme is fixed, regardless of the conventional modulation scheme or the novel hybrid modulation scheme, which makes the system less flexible to accommodate the various access conditions in downlink multiple access. Thus, in this paper, an enhanced ADO-OFDM (eADO-OFDM) scheme is proposed for the first time, in which the numbers of subcarriers occupied by ACO-OFDM and DCO-OFDM can be adaptively adjusted according to the access conditions of services in downlink multiple access. To improve the overall performance of the proposed eADO-OFDM scheme, the following core technologies are investigated.

- In order to achieve the dimming control scheme for the proposed scheme, the enhanced negative ADO-OFDM (eNADO-OFDM) scheme is further introduced based on eADO-OFDM, which is a combination of negative ACO-OFDM (NACO-OFDM) and negative DCO-OFDM (NDCO-OFDM) signals. In eNADO-OFDM, the positive part of the bipolar ACO-OFDM signal is clipped, and the DC bias is subtracted from the bipolar DCO-OFDM signal instead of being added to generate the NDCO-OFDM signal. Then the resulting signal is added to a substantial bias so that the whole signal is still positive and the dynamic range can be fully utilized. Various dimming levels can be achieved by mixing the eADO-OFDM and eNADO-OFDM signals in different appropriate proportions.
- In order to reduce the overall bit error rate (BER), the optimal power allocation under different desired dimming levels is investigated. The BERs of ACO-OFDM and DCO-OFDM are analyzed first. Then, the BER of eADO-OFDM is formulated and the optimal power allocation for eADO-OFDM can be obtained.
- In order to mitigate the impact of the noise and interference during the demodulation process, an iterative receiver with interference cancellation is proposed, in which more accurate estimation of the ACO-OFDM signal can be obtained and the system performance can be improved. Simulation results show that the proposed iterative receiver can achieve superior BER performance compared to the conventional counterparts at the same signal to noise ratio (SNR), while only a few iterations are required for convergence.

The rest of this paper is organized as follows. In Section II, the conventional ADO-OFDM scheme is briefly reviewed. In Section III, the eADO-OFDM scheme with subcarrier assignment is proposed. Then, the transmitting side of eADO-OFDM is illustrated in Section IV, including the dimming control and optimal power allocation schemes. In Section V, the receiving side of eADO-OFDM is investigated, where an iterative receiver with interference cancellation is proposed to reduce the overall BER performance. The simulation results are presented and analyzed in Section VI. Finally, the conclusions are drawn in Section VII.

II. SYSTEM MODEL

In this section, the conventional ADO-OFDM schemes at both transmitting and receiving sides are briefly reviewed. It has been demonstrated that the spectral efficiency of ADO-OFDM is larger than ACO-OFDM, while the overall optical power efficiency is higher than DCO-OFDM [6].

A. THE TRANSMITTING SIDE OF ADO-OFDM

For the ADO-OFDM scheme, odd subcarriers are utilized by the ACO-OFDM signal, while even subcarriers are occupied by the DCO-OFDM signal [10]. Suppose S_k $\left(0 \le k < N/2\right)$ is the symbol modulated on the k-th subcarrier.

For ACO-OFDM, after imposing the Hermitian symmetry to ensure the real values in the time domain, the frequency-domain signal can be written as

$$\mathrm{X}=\left[0,S_1,0,S_3,\cdots,S_{N/2-1},0,S^*_{N/2-1},\cdots,S^*_3,0,S^*_1\right], \quad (1)$$

where $(\cdot)^*$ denotes the operation of conjugation, and N is the number of subcarriers. Then, the bipolar ACO-OFDM signal x_n can be obtained after the operation of N-point inverse fast transform (IFFT), i.e.,

$$x_n = \frac{1}{\sqrt{N}}\sum_{k=0}^{N-1} X_k \exp\left(j\frac{2\pi}{N}nk\right), \quad 0 \le n < N, \quad (2)$$

where X_k denotes the k-th component of X. It has been demonstrated that x_n has antisymmetry property [13], i.e.,

$$x_n = -x_{n+N/2}, \quad 0 \le n < N/2. \quad (3)$$

Thus, the negative portion of x_n can be clipped to zero without any information loss, to leave the non-negative excursions unchanged. Then the unipolar ACO-OFDM signal $x_{aco,n}$ can be given as

$$x_{aco,n} = x_n + n_{aco}, \quad 0 \le n < N, \quad (4)$$

where n_{aco} is the clipping noise of ACO-OFDM signal and can be given by

$$n_{aco} = \begin{cases} -x_n, & x_n \le 0 \\ 0, & x_n > 0. \end{cases} \quad (5)$$

It has been proved that the clipping noise of ACO-OFDM signal will only fall on the even subcarriers, which will not interfere the detection operation of the symbols on the

odd subcarriers. After clipping, the frequency-domain signal of ACO-OFDM on the odd subcarriers can be denoted as

$$X_{aco,k} = \frac{X_k}{2}, \ k \text{ is odd.} \tag{6}$$

For DCO-OFDM, the signal in the frequency domain can be written as

$$\mathrm{Y} = \left[0,0,S_2,0,\cdots,S_{N/2-2},0,0,0,S^*_{N/2-2},\cdots,0,S^*_2,0\right]. \tag{7}$$

Then, the bipolar DCO-OFDM signal y_n can be obtained after the operation of N-point IFFT, i.e.,

$$y_n = \frac{1}{\sqrt{N}} \sum_{k=0}^{N-1} Y_k \exp\left(j\frac{2\pi}{N}nk\right), \quad 0 \le n < N, \tag{8}$$

where Y_k denotes the k-th component of Y. To obtain the non-negative DCO-OFDM signal, a DC bias should be added to y_n and can be formulated as $B_{\mathrm{DC}} = \mu\sqrt{E\left(y_n^2\right)} = \mu\sigma_D$, where μ is a proportional constant and σ_D denotes the standard deviation of the time-domain DCO-OFDM signal, while the metric of B_{DC} and σ_D are Ampere. Like in [14], the bias-index β is defined as $\beta = 10\log_{10}\left(\mu^2+1\right)$ dB. After that, all the remaining negative signals are clipped to zero, leading to the clipping noise n_{dco}, which depends on B_{DC}. Then, the time-domain DCO-OFDM signal $y_{dco,n}$ can be given as

$$y_{dco,n} = y_n + B_{\mathrm{DC}} + n_{dco}, \quad 0 \le n < N, \tag{9}$$

where n_{dco} is the clipping noise of DCO-OFDM signal and can be given by

$$n_{dco} = \begin{cases} -\left(y_n + B_{\mathrm{DC}}\right), & \left(y_n + B_{\mathrm{DC}}\right) \le 0 \\ 0, & \left(y_n + B_{\mathrm{DC}}\right) > 0., \end{cases} \tag{10}$$

which is negligible compared to n_{aco}.

B. THE RECEIVING SIDE OF ADO-OFDM

The transmitted and received ADO-OFDM signals can be formulated by

$$z_{ado,n} = x_{aco,n} + y_{dco,n}, \quad 0 \le n < N, \tag{11}$$

and

$$r_{ado,n} = z_{ado,n} + w_n, \quad 0 \le n < N, \tag{12}$$

respectively, where w_n denotes the thermal noise and shot noise and is modeled as addictive white Gaussian noise (AWGN) in this paper with mean of zero and power spectral density (PSD) of N_0.

The received signal R_k in the frequency domain can be obtained after the process of N-point fast Fourier transform (FFT) based on $r_{ado,n}$, i.e.,

$$R_k = \frac{1}{N} \sum_{n=0}^{N-1} r_{ado,n} \exp\left(-j\frac{2\pi}{N}nk\right), \quad 0 \le k < N. \tag{13}$$

As the clipping operation of ACO-OFDM only affects the data on the even subcarriers, the estimation of ACO-OFDM symbols modulated on the odd subcarriers could be firstly derived as

$$\widehat{X}_k = \underset{X \in \Omega_X}{\operatorname{argmin}} \left\| X - 2R_k \right\|^2, \quad k \text{ is odd}, \tag{14}$$

where Ω_X is the constellation symbol set of ACO-OFDM and $\|\cdot\|$ represents the Frobenius norm. The estimation of the transmitted ACO-OFDM signal $\widehat{x}_{aco,n}$ could be regenerated by $\widehat{X}_k$. Then the estimation of the transmitted DCO-OFDM signal could be denoted by

$$\widehat{y}_{dco,n} = r_{ado,n} - \widehat{x}_{aco,n}. \tag{15}$$

After that, the DC bias is removed and N-point FFT is performed to generate $\widehat{Y}_{dco,k}$, thus the estimation of the DCO-OFDM symbols in the frequency domain could be obtained through

$$\widehat{Y}_k = \underset{Y \in \Omega_Y}{\operatorname{argmin}} \left\| Y - \widehat{Y}_{dco,k} \right\|^2, \quad k \text{ is even}. \tag{16}$$

where Ω_Y is the constellation symbol set of DCO-OFDM. The two parts of the demodulation results $\widehat{X}_k$ and $\widehat{Y}_k$ are combined to obtain the original transmitted symbols. Until now, all the symbols transmitted on the subcarriers are estimated and regenerated.

III. THE EADO-OFDM WITH SUBCARRIER ASSIGNMENT

Since the 0-th and $N/2$-th subcarriers do not transmit signals, ACO-OFDM and DCO-OFDM in conventional ADO-OFDM occupy fixed $N/2$ and $N/2-2$ subcarriers, respectively. A novel modulation scheme with subcarrier assignment for optical wireless communication system, called eADO-OFDM, which can be regarded as an enhanced scheme for conventional ADO-OFDM, is proposed in this section. Compared with the conventional ADO-OFDM scheme, the numbers of subcarriers allocated to ACO-OFDM and DCO-OFDM (including both the information symbols and their corresponding Hermitian symmetries), denoted as N_A and N_D, are not fixed to $N/2$ and $N/2-2$ anymore for eADO-OFDM. Specifically, N_A can be adaptively taken any even number from 0 to $N/2$, while DCO-OFDM occupies the remaining N_D subcarriers, i.e.,

$$\begin{aligned} &N_A + N_D = N - 2, \\ &\text{s.t. } 0 \le N_A \le N/2, \\ &\quad N/2 - 2 \le N_D \le N - 2. \end{aligned} \tag{17}$$

One of the advantages for eADO-OFDM is that the numbers of subcarriers allocated to ACO-OFDM and DCO-OFDM can be adaptively adjusted according to different optimization objectives. For example, on the perspective of the access conditions of services in downlink multiple access, services with low complexity and/or low latency could adopt ACO-OFDM for transmission so that they can be preferentially demodulated, while DCO-OFDM could be allocated to the rest services which are with low requirement for complexity and latency.

For eADO-OFDM, the transmitted signal can be obtained in the same manner as that of the conventional ADO-OFDM. Because the ACO-OFDM signal in eADO-OFDM still only occupies the odd subcarriers, the ACO-OFDM and DCO-OFDM signals can be detected in the same way as the conventional ADO-OFDM scheme.

Moreover, to effectively achieve the dimming control scheme, eNADO-OFDM is firstly imposed in this paper to the best of our knowledge, which is a combination of NACO-OFDM and NDCO-OFDM signals. For NACO-OFDM, the operations are the same as those in ACO-OFDM before asymmetrical clipping, while the positive part of x_n is clipped without loss of information according to (3) to leave the non-positive excursions unchanged. Then the NACO-OFDM signal $x_{naco,n}$ in time domain can be represented as

$$x_{naco,n} = x_n + n_{naco}, \quad 0 \le n < N, \tag{18}$$

where n_{naco} is the clipping noise of NACO-OFDM signal in eNADO-OFDM, which is given by

$$n_{naco} = \begin{cases} 0, & x_n < 0 \\ -x_n, & x_n \ge 0. \end{cases} \tag{19}$$

For NDCO-OFDM, the DC bias is subtracted from y_n instead of being added. After that, all the remaining positive signals are clipped to zero, leading to the clipping noise n_{ndco} i.e.,

$$y_{ndco,n} = y_n - B_{\mathrm{DC}} + n_{ndco}, \tag{20}$$

and

$$n_{ndco} = \begin{cases} 0, & (y_n - B_{\mathrm{DC}}) \le 0 \\ -(y_n - B_{\mathrm{DC}}), & (y_n - B_{\mathrm{DC}}) > 0. \end{cases} \tag{21}$$

Thus, the transmitted and received eNADO-OFDM signals can be formulated by

$$z_{nado,n} = x_{naco,n} + y_{ndco}, \quad 0 \le n < N, \tag{22}$$

and

$$r_{nado,n} = z_{nado,n} + w_n, \quad 0 \le n < N, \tag{23}$$

respectively. It can be observed that the bipolar ACO-OFDM signal x_n is divided into two unipolar signals $x_{aco,n}$ and $x_{naco,n}$ after different kinds of clippings, resulting in two kinds of signals in the frequency domain. Thus, the original ACO-OFDM signal in the frequency domain can be combined with these two kinds of signals, i.e.,

$$X_k = X_{aco,k} + X_{naco,k}. \tag{24}$$

From (6) and (24), it is easy to be derived that

$$X_{naco,k} = \frac{X_k}{2}, \quad k \text{ is odd}. \tag{25}$$

Hence, at the receiver of eNADO-OFDM, the NACO-OFDM signal and NDCO-OFDM signal can be detected in the same manner as the ACO-OFDM signal and DCO-OFDM signal in the eADO-OFDM scheme, respectively, except that the positive part of bipolar ACO-OFDM signal is clipped in the regeneration process, and the DC bias should be added instead of being subtracting to obtain the estimated bipolar DCO-OFDM.

Like eADO-OFDM, in the eNADO-OFDM scheme, the number of subcarriers allocated to NACO-OFDM and NDCO-OFDM can be also flexibly adjusted according to different optimization objectives, thereby improving the system adaptability.

IV. THE TRANSMITTING SIDE OF EADO-OFDM

In this section, dimming control schemes for eADO-OFDM is investigated to support different dimming levels. After that, the power allocation scheme under a desired dimming level is proposed to reduce the overall BER.

A. DIMMING CONTROL FOR THE PROPOSED EADO-OFDM SYSTEM

Communication capabilities of VLC systems under dimmable illumination should be taken into consideration to accommodate different illuminance demands [15]. Dimming control is essential to support different dimming levels in VLC system, and has been studied by many researchers. For DCO-OFDM systems, different dimming levels are achieved by adding different DC bias to adjust the average amplitude of the transmitted signal, so that the luminance of LEDs can be changed. However, when the desired dimming level is very high or low, the system performance will be sacrificed because of the restricted dynamic range of the LEDs [16]. Thus, a piecewise function is imposed to solve this problem [17]. In [18], an asymmetric hybrid optical OFDM (AHO-OFDM) system is investigated, where ACO-OFDM and reverse PAM-DMT are applied for odd subcarriers and even subcarriers, respectively, while a DC bias is used to support various dimming targets. Nevertheless, the demodulation operation is sensitive to the DC bias due to that the scaling factors of both ACO-OFDM and PAM-DMT depend on the dimming level. Various dimming levels can be achieved by adjusting the appropriate ratio of the negative HACO-OFDM (NHACO-OFDM) and HACO-OFDM signals in [19]. However, only the imaginary part of the subcarrier is utilized in PAM-DMT, resulting in the degradation of the spectral efficiency.

In this paper, the eADO-OFDM signal is applied when a low dimming level is requested, while the eNADO-OFDM signal is utilized when a high dimming level is required. And the intermediate dimming levels are achieved by adjusting the proportion of the eADO-OFDM and eNADO-OFDM signals. Because of the nonlinear transfer characteristic of LEDs, the transmitted signal should be restricted in a limited dynamic range to ensure the communication quality [4]. Assume the limited dynamic range of LEDs is between I_L and I_H, where I_L and I_H represent the minimum and maximum allowed current values to ensure the approximately linear transfer characteristic, respectively, resulting in the

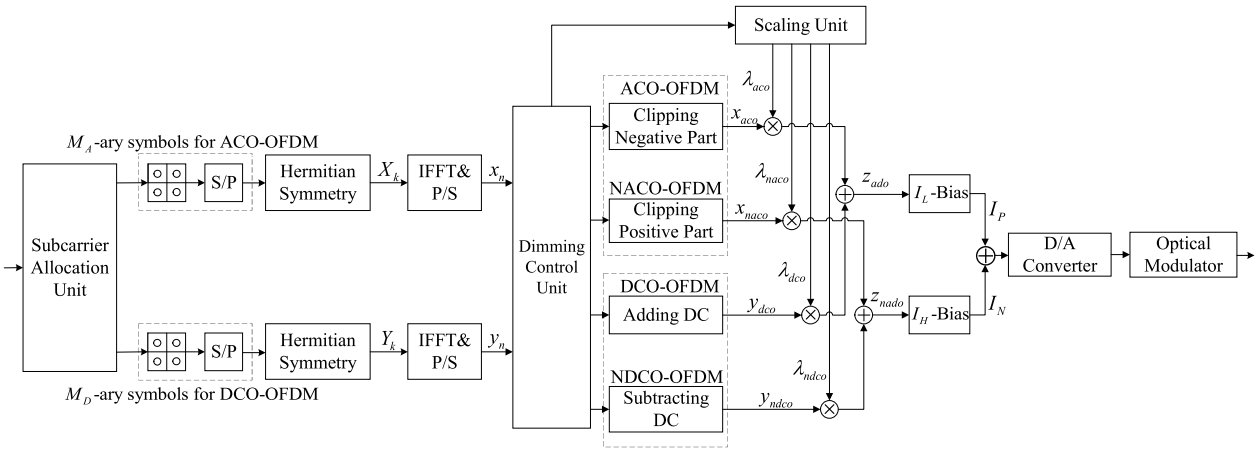

FIGURE 1. The structure diagram of the proposed dimmable eADO-OFDM transmitter.

LED dynamic range of $I_H - I_L$, during which the transfer characteristic of LEDs can be regarded as linear.

The transmitter structure of the proposed VLC system with dimming control is shown in Fig. 1. First, the subcarriers occupied by ACO-OFDM and DCO-OFDM is determined by the subcarrier allocation unit. Then, after performing the constellation mapping, serial-to-parallel (S/P), Hemitian symmetry imposing, IFFT, and parallel-to-serial (P/S) operations, the bipolar x_n and y_n are obtained. Then the negative or positive part of x_n is clipped and multiplied by scaling factors λ_{aco} and λ_{naco}, respectively, which is determined by the dimming control unit. At the same time, the DC bias is added or subtracted from y_n to generate unipolar y_{dco} and y_{ndco}. Similarly, y_{dco} and y_{ndco} are also multiplied by scaling factors λ_{dco} and λ_{ndco}, respectively. Note the scaling factors are imposed to achieve the demanded dimming level, while the entire dynamic range of LEDs can be exploited. Then the eADO-OFDM signal z_{ado} or eNADO-OFDM signal z_{nado} can be obtained with a specific proportion, which is adaptively decided by the dimming control unit. Next, DC bias I_L and I_H are added to the eADO-OFDM and eNADO-OFDM signals, respectively, to make sure that the transmitted signal is non-negative. The eADO-OFDM and eNADO-OFDM signals with DC bias are mixed and passed through a digital to analog (D/A) converter and then modulates the optical intensity for transmission. At the receiver, the corresponding reverse operations are performed based on the received signal.

Without loss of generality, assume that $\lambda_{aco} = \lambda_{naco} = \lambda_{dco} = \lambda_{ndco} = \lambda$. Thus, the eADO-OFDM and eNADO-OFDM signals can be given by

$$I_P = I_L + z_{ado,n} = I_L + \lambda\left(x_{aco,n} + y_{dco,n}\right), \tag{26}$$

and

$$I_N = I_H + z_{nado,n} = I_H + \lambda\left(x_{naco,n} + y_{ndco,n}\right), \tag{27}$$

respectively.

The probability density functions (PDFs) of ACO-OFDM and DCO-OFDM have been investigated in [6], which can be formulated as

$$f_{x_{aco}}(\omega) = \frac{1}{\sqrt{2\pi}\sigma_A}\exp\left(\frac{-\omega^2}{2\sigma_A^2}\right)u(\omega) + \frac{1}{2}\delta(\omega), \tag{28}$$

and

$$f_{y_{dco}}(\omega) = \frac{1}{\sqrt{2\pi}\sigma_D}\exp\left(\frac{-(\omega - B_{\mathrm{DC}})^2}{2\sigma_D^2}\right)u(\omega) + Q\left(\frac{B_{\mathrm{DC}}}{\sigma_D}\right)\delta(\omega), \tag{29}$$

respectively, where σ_A^2 is the variance of the unclipped ACO-OFDM signal in the time domain, $Q(x) = 1/\sqrt{2\pi}\cdot\int_x^{\infty}\exp\left(-u^2/2\right)\mathrm{d}u$, and $u(\cdot)$ and $\delta(\cdot)$ denote the unit-step and Dirac delta functions, respectively.

Through the PDFs, the optical power of ACO-OFDM and DCO-OFDM in conventional ADO-OFDM can be represented as

$$P_{ACO,o} = \frac{\sigma_A}{\sqrt{2\pi}}, \tag{30}$$

and

$$P_{DCO,o} = \sigma_D\left\{\mu\left[1 - Q(\mu)\right] + \frac{1}{\sqrt{2\pi}}\exp\left(-\frac{\mu^2}{2}\right)\right\}, \tag{31}$$

respectively [20].

Thus, in the proposed eADO-OFDM, the expectations of ACO-OFDM and DCO-OFDM signals can be calculated through (30) to (31) and can be formulated as

$$P_{eACO,o} = E(x_{aco}) = \sqrt{\frac{N_A}{N}}\cdot\frac{\delta_A}{\sqrt{2\pi}}, \tag{32}$$

and

$$P_{eDCO,o} = E(y_{dco}) = \sqrt{\frac{N_D}{N}}\cdot D\delta_D, \tag{33}$$

respectively, according to the Parseval's theorem [21], where δ_A^2 and δ_D^2 represent the electrical energy per subcarrier for ACO-OFDM and DCO-OFDM, respectively, and

$D = \mu\left(1 - Q\left(\mu\right)\right) + 1/\sqrt{2\pi} \cdot \exp\left(-\mu^2/2\right)$. Then, the average amplitudes of I_P and I_N can be calculated as

$$A_P = I_L + \lambda\left(\sqrt{\frac{N_A}{N}} \cdot \frac{\delta_A}{\sqrt{2\pi}} + \sqrt{\frac{N_D}{N}} \cdot D\delta_D\right), \tag{34}$$

and

$$A_N = I_H - \lambda\left(\sqrt{\frac{N_A}{N}} \cdot \frac{\delta_A}{\sqrt{2\pi}} + \sqrt{\frac{N_D}{N}} \cdot D\delta_D\right), \tag{35}$$

respectively. In order to verify the dimming performance of the proposed system, a parameter η called the dimming level is defined as

$$\eta = \frac{A - I_L}{I_H - I_L}. \tag{36}$$

where A denotes the average amplitude of transmitted signal.

The I_N signal is used when a high η is desired, while the I_P signal is utilized for a low η. Under these two circumstances, dimming control is achieved by adjusting the power allocation for ACO-OFDM and DCO-OFDM. When an intermediate η is desired, the transmitted signal is an algebraic sum of the I_N and I_P signals. That means, the I_N and I_P signals are combined with a proper proportion. Suppose the ratio of I_P signal is α, thus the average amplitude A of the combined signal is denoted as

$$A = \alpha A_P + (1 - \alpha) A_N. \tag{37}$$

In this case, the dimming control scheme can be achieved by adaptively adjusting α to the required A, while the dynamic range of LEDs can be fully exploited, thus high power efficiency can be ensured under this circumstance.

B. POWER ALLOCATION SCHEME FOR THE PROPOSED EADO-OFDM SYSTEM

Several power allocation schemes for OFDM-based optical wireless communication systems have been investigated. For example, in [22], an optimal power allocation scheme with optical power constraints based on the principle of effective signal to noise ratio optimum is investigated to reduce the nonlinear clipping distortion of ACO-OFDM. For DCO-OFDM system, the information-carrying power and DC-offset power are jointly analyzed and optimized to take a tradeoff of the power consumption and clipping distortion [23]. The optimal power allocation factor for both ACO-OFDM and DCO-OFDM signals in ADO-OFDM under the normalized total optical power is investigated in [24]. However, both subcarrier assignment and dimming control are not considered in all the above power allocation schemes to the best of our knowledge.

Thus a power allocation scheme for the proposed eADO-OFDM scheme with subcarrier assignment to reduce the overall BER is investigated under a desired dimming level in this section. Without loss of generality, quadrature amplitude modulation (QAM) is assumed for both ACO-OFDM and DCO-OFDM, while the constellation orders are M_A and M_D, respectively. When Gray labeling is applied, the BER performance of ACO-OFDM with scaling factor λ in the eADO-OFDM can be given as [25]

$$B_{e,ACO} = \frac{4\left(\sqrt{M_A} - 1\right)}{\sqrt{M_A}\log_2 M_A} Q\left(\sqrt{\frac{3}{M_A - 1}\frac{\lambda^2\delta_A^2}{4N_0}}\right). \tag{38}$$

Then, the BER performance of DCO-OFDM in the eADO-OFDM can be derived as

$$\begin{aligned} B_{e,DCO} &= B_{e,ACO}B_{e,DCO|\overline{ACO}} + \left(1 - B_{e,ACO}\right) B_{e,DCO|ACO} \\ &= B_{e,DCO|ACO} + B_{e,ACO}\left(B_{e,DCO|\overline{ACO}} - B_{e,DCO|ACO}\right), \end{aligned} \tag{39}$$

where $B_{e,DCO|\overline{ACO}}$ and $B_{e,DCO|ACO}$ denote the conditional probability of error given that the ACO-OFDM signal has been demodulated wrongly and successfully, respectively. Generally, under high SNR, $B_{e,ACO}$, $B_{e,DCO|\overline{ACO}}$ and $B_{e,DCO|ACO}$ could be small, thus the second term in (39) is much smaller than $B_{e,DCO|ACO}$ and could be neglected. Hence, equation (39) is approximately estimated as

$$\begin{aligned} B_{e,DCO} &= B_{e,DCO|ACO} \\ &= \frac{4\left(\sqrt{M_D} - 1\right)}{\sqrt{M_D}\log_2 M_D} Q\left(\sqrt{\frac{3}{M_D - 1}\frac{\lambda^2\delta_D^2}{N_0}}\right). \end{aligned} \tag{40}$$

Therefore, the overall BER performance of eADO-OFDM can be derived as

$$\begin{aligned} B_{e,ADO} &= \frac{N_A\log_2 M_A B_{e,ACO} + N_D\log_2 M_D B_{e,DCO}}{N_A\log_2 M_A + N_D\log_2 M_D} \\ &= \frac{4N_A\left(\sqrt{M_A} - 1\right) Q\left(\frac{\lambda\delta_A}{2}\sqrt{\frac{3}{(M_A - 1)N_0}}\right)}{\sqrt{M_A}\left(N_A\log_2 M_A + N_D\log_2 M_D\right)} \\ &\quad + \frac{4N_D\left(\sqrt{M_D} - 1\right) Q\left(\lambda\delta_D\sqrt{\frac{3}{(M_D - 1)N_0}}\right)}{\sqrt{M_D}\left(N_A\log_2 M_A + N_D\log_2 M_D\right)}. \end{aligned} \tag{41}$$

The pure eADO-OFDM signal is applied when the dimming level is low, denoted as η_l. Thus the optimization objective when low dimming level is desired can be given as

$$\begin{aligned} &\min_{\lambda\delta_A, \lambda\delta_D} B_{e,ADO} \\ &\text{s.t. } \eta = \eta_l. \end{aligned} \tag{42}$$

According to (34) and (36), it can be derived that

$$\sqrt{\frac{N_A}{2\pi N}}\lambda\delta_A + \sqrt{\frac{N_D}{N}} \cdot D\lambda\delta_D = \eta_l\left(I_H - I_L\right), \tag{43}$$

where the left two terms are the optical power of ACO-OFDM and DCO-OFDM in the eADO-OFDM scheme, respectively, as described by (32) and (33). And the right term of (43) represents the total optical power $P_{o,ADO}$ of the eADO-OFDM scheme. Thus, if the ratio of the optical power for ACO-OFDM to the total optical power is $\rho \in (0, 1)$, the optical power of ACO-OFDM and DCO-OFDM can be denoted as $\rho\eta_l(I_H - I_L)$ and $(1 - \rho)\eta_l(I_H - I_L)$, which can be derived as

$$\sqrt{\frac{N_A}{2\pi N}}\lambda\delta_A = \rho\eta_l\left(I_H - I_L\right), \tag{44}$$

and

$$\sqrt{\frac{N_D}{N}} \cdot D\lambda\delta_D = (1-\rho)\,\eta_l\,(I_H - I_L). \tag{45}$$

respectively. After inserting (44) and (45) into (41), the derivative of (41) can be derived as

$$\begin{aligned} B'_{e,ADO} &= \frac{4N_A\left(\sqrt{M_A}-1\right)\eta_l\,(I_H-I_L)}{\sqrt{M_A}\left(N_A\log_2 M_A + N_D\log_2 M_D\right)} \times \sqrt{\frac{3\pi N}{2N_0N_A(M_A-1)}} \\ &\quad \times Q'\left(\rho\eta_l\,(I_H-I_L)\sqrt{\frac{3\pi N}{2N_0N_A(M_A-1)}}\right) \\ &\quad - \frac{4N_D\left(\sqrt{M_D}-1\right)\eta_l\,(I_H-I_L)}{\sqrt{M_D}\left(N_A\log_2 M_A + N_D\log_2 M_D\right)D}\sqrt{\frac{3N}{N_0N_D(M_D-1)}} \\ &\quad \times Q'\left(\frac{(1-\rho)\,\eta_l\,(I_H-I_L)}{D}\sqrt{\frac{3N}{N_0N_D\,(M_D-1)}}\right), \end{aligned} \tag{46}$$

where $Q'(x) = -1/\sqrt{2\pi}\exp\left(-x^2/2\right)$, and the second derivative of (41) can be derived as

$$\begin{aligned} B''_{e,ADO} &= \frac{6\pi N\eta_l^2(I_H-I_L)^2\left(\sqrt{M_A}-1\right)}{N_0\,(M_A-1)\sqrt{M_A}\left(N_A\log_2 M_A + N_D\log_2 M_D\right)} \\ &\quad \times Q''\left(\rho\eta_l\,(I_H-I_L)\sqrt{\frac{3\pi N}{2N_0N_A\,(M_A-1)}}\right) \\ &\quad + \frac{12N\eta_l^2(I_H-I_L)^2\left(\sqrt{M_D}-1\right)}{N_0\,(M_D-1)\sqrt{M_D}\left(N_A\log_2 M_A + N_D\log_2 M_D\right)D^2} \\ &\quad \times Q''\left(\frac{(1-\rho)\,\eta_l\,(I_H-I_L)}{D}\sqrt{\frac{3N}{N_0N_D\,(M_D-1)}}\right), \end{aligned} \tag{47}$$

where $Q''(x) = x/\sqrt{2\pi}\exp\left(-x^2/2\right) > 0$ for $x > 0$. Thus, for $0 < \rho < 1$, it can be derived that $B''_{e,ADO} > 0$, which indicates that $B_{e,ADO}$ is a convex function of ρ. Hence, the ρ_0 to minimize $B_{e,ADO}$ can be calculated ba setting $B'_{e,ADO} = 0$, which can be represented as

$$\begin{aligned} \rho_0(\eta_l) &= \frac{-\frac{N}{N_D} + \sqrt{\frac{\pi N^2D^2(M_D-1)}{2N_AN_D(M_A-1)} + \left[\frac{\pi ND^2(M_D-1)}{2N_A(M_A-1)} - \frac{N}{N_D}\right]G(\eta_l)}}{\frac{\pi ND^2(M_D-1)}{2N_A(M_A-1)} - \frac{N}{N_D}}, \end{aligned} \tag{48}$$

where G is given by

$$G(\eta_l) = \frac{2D^2N_0\,(M_D-1)}{3\eta_l^2(I_H-I_L)^2}\ln\left[\frac{D\sqrt{\pi N_A}\left(\sqrt{M_A}-1\right)\sqrt{M_D^2-M_D}}{\sqrt{2N_D}\left(\sqrt{M_D}-1\right)\sqrt{M_A^2-M_A}}\right]. \tag{49}$$

Then, the optimal power allocation can be calculated as

$$\delta_{Ao}(\eta_l) = \frac{\rho_0(\eta_l)\,\eta_l\,(I_H-I_L)}{\lambda}\sqrt{\frac{2\pi N}{N_A}}, \tag{50}$$

and

$$\delta_{Do}(\eta_l) = \frac{(1-\rho_0(\eta_l))\,\eta_l\,(I_H-I_L)}{\lambda D}\sqrt{\frac{N}{N_D}}, \tag{51}$$

according to (44) and (45). It is worth noting that the BER performance of ACO-OFDM and NACO-OFDM is quite the same according to (3). Moreover, the BER of DCO-OFDM is equal to that of NDCO-OFDM because that the DC component will not impact the BER performance. Hence, the BERs of eADO-OFDM and eNADO-OFDM are also the same, i.e., $B_{e,NADO} = B_{e,ADO}$.

Similarly, the pure eNADO-OFDM signal is applied when the dimming level is high, denoted as η_h. Thus the optimization objective when high dimming level is desired can be given as

$$\begin{aligned} &\min_{\lambda\delta_A,\lambda\delta_D} B_{e,NADO} \\ &\text{s.t. } \eta = \eta_h. \end{aligned} \tag{52}$$

The optimal power allocation under a high dimming level can be obtained by the same mathematic means as that under a low dimming level, and can be formulated as

$$\delta_{Ao}(\eta_h) = \frac{\rho_0\,(1-\eta_h)(1-\eta_h)\,(I_H-I_L)}{\lambda}\sqrt{\frac{2\pi N}{N_A}}, \tag{53}$$

and

$$\delta_{Do}(\eta_h) = \frac{(1-\rho_0\,(1-\eta_h))\,(1-\eta_h)\,(I_H-I_L)}{\lambda D}\sqrt{\frac{N}{N_D}}. \tag{54}$$

For the intermediate dimming level which is a combination of eADO-OFDM an eNADO-OFDM signals, the overall BER can be formulated as

$$B_{e,m} = \alpha B_{e,ADO} + (1-\alpha)\,B_{e,NADO} = B_{e,ADO}. \tag{55}$$

Because the intermediate dimming levels are achieved by adjusting the proportion α, the optimization constraint under this circumstance is the clipping ratio instead of the dimming level anymore, which is formulated as

$$\begin{aligned} &\min_{\lambda\delta_A,\lambda\delta_D} B_{e,m} \\ &\text{s.t.} \int_0^{I_H-I_L} f_{z_{ado}}(\omega)d\omega \geq 1-\varepsilon, \end{aligned} \tag{56}$$

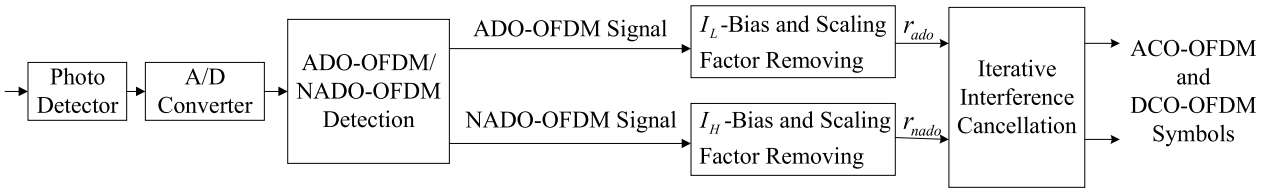

FIGURE 2. The structure diagram of the proposed dimmable eADO-OFDM receiver.

where ε is the desired clipping ratio and $f_{z_{ado}}(\omega)$ is the PDF of eADO-OFDM with scaling factor λ and can be given by

$$\begin{aligned} & f_{z_{ado}}(\omega) \\ &= \frac{\sqrt{N}\exp\left(\frac{-N(\omega-B_{\mathrm{DC}})^2}{2\lambda^2\left(N_D\delta_D^2+N_A\delta_A^2\right)}\right)}{\lambda\sqrt{2\pi\left(N_D\delta_D^2+N_A\delta_A^2\right)}} \\ &\quad\times\left\{Q\left[\frac{-\sqrt{N}\left(\omega N_D\delta_D^2+B_{\mathrm{DC}}N_A\delta_A^2\right)}{\lambda\delta_A\delta_D\sqrt{N_AN_D\left(N_D\delta_D^2+N_A\delta_A^2\right)}}\right]\right. \\ &\quad\left.-Q\left[\frac{\sqrt{N}\left(\omega N_A\delta_A^2-B_{\mathrm{DC}}N_A\delta_A^2\right)}{\lambda\delta_A\delta_D\sqrt{N_AN_D\left(N_D\delta_D^2+N_A\delta_A^2\right)}}\right]\right\}+\frac{\sqrt{N}}{\lambda\sqrt{2\pi}} \\ &\quad\times\left[\frac{1}{\delta_A\sqrt{N_A}}\exp\left(\frac{-N\omega^2}{2N_A\lambda^2\delta_A^2}\right)Q\left(\frac{B_{\mathrm{DC}}\sqrt{N}}{\lambda\delta_D\sqrt{N_D}}\right)+\frac{1}{2\delta_D\sqrt{N_D}}\right. \\ &\quad\left.\times\exp\left(\frac{-N(\omega-B_{\mathrm{DC}})^2}{2N_D\lambda^2\delta_D^2}\right)\right]u(\omega)+\frac{Q\left(\frac{\sqrt{N}B_{\mathrm{DC}}}{\sqrt{N_D}\lambda\delta_D}\right)\delta(\omega)}{2}, \end{aligned} \tag{57}$$

where $\otimes$ represents the operation of convolution.

V. THE RECEIVING SIDE OF EADO-OFDM

Some demodulation schemes for OFDM-based VLC systems have been proposed. For DCO-OFDM, an iterative detection algorithm is proposed with a power-efficient symbol recovery scheme [14]. In [26], a pairwise maximum likelihood (ML) detector which exploits the anti-symmetry of time-domain ACO-OFDM samples is proposed to improve the optical power efficiency. Based on this, an iterative receiver to reduce the effect of noise and estimation error is investigated in [24]. In [27], a receiver for HACO-OFDM systems is introduced by utilizing the characteristic of both ACO-OFDM and PAM-DMT signals in the time domain to reduce the clipping noise of ACO-OFDM and avoid the error propagation.

In this section, a novel iterative receiver for the proposed eADO-OFDM scheme to mitigate the impact of noise and interference is investigated. Specifically, the receiver structure of the proposed dimmable eADO-OFDM receiver is illustrated in Fig. 2. After receiving a frame, it is necessary to distinguish whether eADO-OFDM or eNADO-OFDM is adopted. It can be seen from Fig. 3 that there is a gap between the average amplitudes A_P and A_N, thus the two modulation

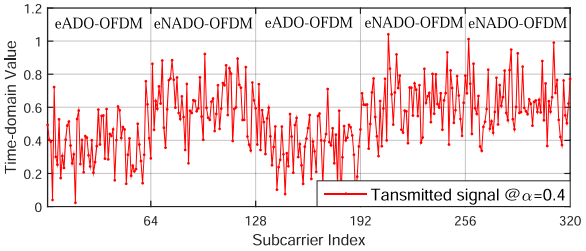

FIGURE 3. Waveform of the mixed transmitted signal at $\alpha = 0.4$.

schemes can be distinguished by the average amplitude, where the threshold is given by

$$A_d = \frac{A_P + A_N}{2} = \frac{I_L + I_H}{2}. \tag{58}$$

When the average amplitude of the received frame is greater than A_d, it is regarded as a frame of eNADO-OFDM, otherwise, it is judged to be a frame of eADO-OFDM. There are also some other distinction methods, for example, one of the occupied subcarriers can be utilized to indicate whether eADO-OFDM or eNADO-OFDM is applied.

Suppose the indexes of the occupied subcarriers by ACO-OFDM and DCO-OFDM, denoted as $\boldsymbol{\zeta}_{aco}$ and $\boldsymbol{\zeta}_{aco}$, are known at the receiver. For eADO-OFDM, since ACO-OFDM signal only occupies the odd subcarriers, the clipping noise of ACO-OFDM signal will still only fall on the even subcarriers. Thus, the ACO-OFDM and DCO-OFDM signals can be demodulated in the same way as the conventional ADO-OFDM.

Based on this, an iterative receiver with interference cancellation, in which the pairwise averaging and pairwise clipping are exploited, is proposed in this paper to further mitigate the impact of noise and interference. In essence, the demodulation processes for eADO-OFDM and eNADO-OFDM are the same, except the clipping and DC-removing operations. Thus, this section takes eADO-OFDM as an example to describe the proposed iterative interference cancellation scheme, which is shown in Fig. 4.

To decrease the effect of noise, the pairwise averaging is imposed first, which utilizes the Hermitian symmetry of the transmitted frequency-domain signal. For $k < N/2$ and $k \in \boldsymbol{\zeta}_{aco}$, the combined frequency-domain signal can be formulated as

$$R_k^a = \mathrm{Re}\left(\frac{R_k + R_{N-k}}{2}\right) + j\mathrm{Im}\left(\frac{R_k - R_{N-k}}{2}\right), \tag{59}$$

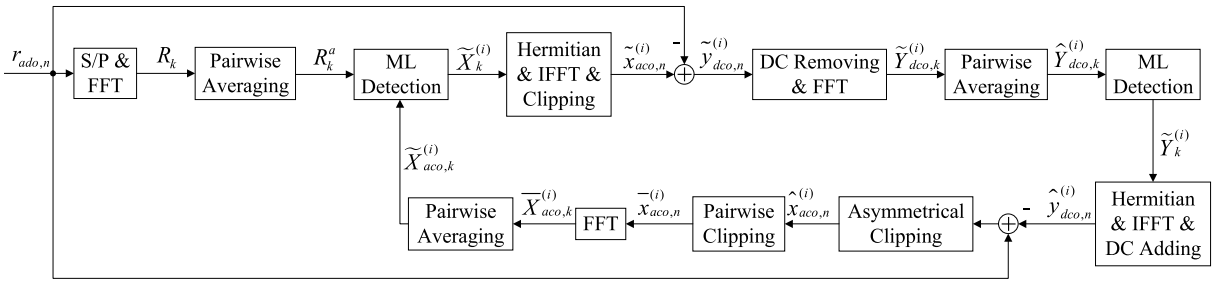

FIGURE 4. The structure diagram of the proposed iterative interference cancellation scheme.

where $\mathrm{Re}(\cdot)$ and $\mathrm{Im}(\cdot)$ denote the real part and imaginary part, respectively, and $j^2 = -1$. After that, the iteration process begins at the ML detection unit, and the iteration process is performed as follows.

1) ESTIMATE ACO-OFDM SYMBOLS

Consider the i-th iteration, the estimation of ACO-OFDM symbols can be obtained by the ML criterion as

$$\widetilde{X}_k^{(i)} = \underset{X\in\Omega_X}{\operatorname{argmin}} ||X - 2\widetilde{X}_{aco,k}^{(i-1)}||^2, \quad k \in \boldsymbol{\zeta}_{aco}, \tag{60}$$

where $\widetilde{X}_{aco,k}^{(0)} = R_k^a$.

2) REGENERATE THE DCO-OFDM SIGNAL

Specifically, the estimation of the time-domain ACO-OFDM signal $\widetilde{x}_{aco,n}^{(i)}$ is regenerated by $\widetilde{X}_k^{(i)}$. Next, the estimation of the time-domain DCO-OFDM signal can be obtained by

$$\widetilde{y}_{dco,n}^{(i)} = r_{ado,n} - \widetilde{x}_{aco,n}^{(i)}. \tag{61}$$

Then the DC bias is removed from $\widetilde{y}_{dco,n}^{(i)}$, and N-point FFT is performed to generate the frequency-domain DCO-OFDM signal $\widetilde{Y}_{dco,k}^{(i)}$.

3) CALCULATE THE ESTIMATION OF DCO-OFDM SYMBOLS

The pairwise averaging is imposed for $k < N/2$ and $k \in \boldsymbol{\zeta}_{dco}$ to reduce the impact of noise, which is given as

$$\widehat{Y}_{dco,k}^{(i)} = \mathrm{Re}\left(\frac{\widetilde{Y}_{dco,k}^{(i)} + \widetilde{Y}_{dco,N-k}^{(i)}}{2}\right) + j\mathrm{Im}\left(\frac{\widetilde{Y}_{dco,k}^{(i)} - \widetilde{Y}_{dco,N-k}^{(i)}}{2}\right). \tag{62}$$

Then the estimation of the DCO-OFDM symbols can be represented as

$$\widetilde{Y}_k^{(i)} = \underset{Y\in\Omega_Y}{\operatorname{argmin}} \|Y - \widehat{Y}_{dco,k}^{(i)}\|^2, \quad k \in \boldsymbol{\zeta}_{dco}. \tag{63}$$

4) MITIGATE INTERFERENCE BASED ON PAIRWISE CLIPPING

First, the time-domain DCO-OFDM signal $\widehat{y}_{dco,n}^{(i)}$ is regenerated and subtracted from $r_{ado,n}$. Then, the time-domain ACO-OFDM signal $\widehat{x}_{aco,n}^{(i)}$ can be regenerated after asymmetrical clipping. Note that one of the original time-domain ACO-OFDM signals on the n-th and $(n+N/2)$-th subcarriers must be zero after asymmetrical clipping according to (4) and (5). Based on this, the pairwise clipping is imposed in this paper, which can reduce the impact of noise and interference. Hence, the more accurate estimation of time-domain ACO-OFDM signal is given as

$$\overline{x}_{aco,n}^{(i)} = \begin{cases} 0, & \widehat{x}_{aco,n}^{(i)} < \widehat{x}_{aco,n+N/2}^{(i)} \\ \widehat{x}_{aco,n}^{(i)} & , \widehat{x}_{aco,n}^{(i)} \geq \widehat{x}_{aco,n+N/2}^{(i)}, \end{cases} \tag{64}$$

and

$$\overline{x}_{aco,n+N/2}^{(i)} = \begin{cases} \widehat{x}_{aco,n+N/2}^{(i)}, & \widehat{x}_{aco,n}^{(i)} < \widehat{x}_{aco,n+N/2}^{(i)} \\ 0, & \widehat{x}_{aco,n}^{(i)} \geq \widehat{x}_{aco,n+N/2}^{(i)}, \end{cases} \tag{65}$$

where $n = 0, 1, \ldots, N/2-1$.

5) UPDATE THE ACO-OFDM SIGNAL

After N-point FFT, $\overline{X}_{aco,k}^{(i)}$ is obtained. Then, the pairwise averaging is imposed for $k < N/2$ and $k \in \boldsymbol{\zeta}_{aco}$, which is given as

$$\widetilde{X}_{aco,k}^{(i)} = \mathrm{Re}\left(\frac{\overline{X}_{aco,k}^{(i)} + \overline{X}_{aco,N-k}^{(i)}}{2}\right) + j\mathrm{Im}\left(\frac{\overline{X}_{aco,k}^{(i)} - \overline{X}_{aco,N-k}^{(i)}}{2}\right). \tag{66}$$

With that, an entire iteration process has been completed. The same operations are performed iteratively to obtain more accurate estimation of the original ACO-OFDM and DCO-OFDM symbols until the maximum number of iterations T is reached or the BER is less than τ, as shown in **Algorithm 1**.

VI. SIMULATION RESULTS

Simulation results are performed to evaluate the performance of the proposed scheme. System parameters are listed in Table 1.

The dimming level η as a function of ratio α is illustrated in Fig. 5, while N_A varies from 16 to 64 and the bias-index β is set as 10 dB. It can be seen from the figure that the dimming level decreases with the increase of ratio α, and a wide dimming range can be ensured by the proposed dimming control scheme. For example, the achievable dimming range is from 21% to 79% when $N_A = 16$. Moreover, the dimming range could be further stretched along with the increase of N_A even if the desired dimming level η_l or η_h is extremely

Algorithm 1 Iterative Interference Cancellation Scheme for eADO-OFDM

Require:

1) Error threshold τ,
2) Received signal r_{ado},
3) Constellation symbol sets Ω_X and Ω_Y,
4) Maximum number of iterations T.

Initialization:

$\widetilde{X}_k^{(0)} \leftarrow$ a random symbol in Ω_X,
$\widetilde{Y}_k^{(0)} \leftarrow$ a random symbol in Ω_Y,
Calculate R_k^a based on r_{ado},
$\widetilde{X}_{aco,k}^{(0)} \leftarrow R_k^a$, $\mathrm{BER}^{(0)} \leftarrow 1$, $i \leftarrow 1$,

Iterations:

repeat
  $\widetilde{X}_k^{(i)} \leftarrow \underset{X\in\Omega_X}{\operatorname{argmin}} ||X - 2\widetilde{X}_{aco,k}^{(i-1)}||^2$,
  Regenerate $\widetilde{x}_{aco,n}^{(i)}$, $\widetilde{y}_{dco,n}^{(i)} \leftarrow r_{ado,n} - \widetilde{x}_{aco,n}^{(i)}$, produce $\widetilde{Y}_{dco,k}^{(i)}$ after DC removing and N-point FFT,
  $\widehat{Y}_{dco,k}^{(i)} \leftarrow \mathrm{Re}\left(\frac{\widetilde{Y}_{dco,k}^{(i)} + \widetilde{Y}_{dco,N-k}^{(i)}}{2}\right) + j\mathrm{Im}\left(\frac{\widetilde{Y}_{dco,k}^{(i)} - \widetilde{Y}_{dco,N-k}^{(i)}}{2}\right)$, $\widetilde{Y}_k^{(i)} \leftarrow \underset{Y\in\Omega_Y}{\operatorname{argmin}} ||Y - \widehat{Y}_{dco,k}^{(i)}||^2$,
  Calculate $\widehat{y}_{dco,n}^{(i)}$, generate $\widehat{x}_{aco,n}^{(i)}$,
  if $\widehat{x}_{aco,n}^{(i)} < \widehat{x}_{aco,n+N/2}^{(i)}$ **then**
    $\overline{x}_{aco,n}^{(i)} \leftarrow 0$, $\overline{x}_{aco,n+N/2}^{(i)} \leftarrow \widehat{x}_{aco,n+N/2}^{(i)}$,
  else
    $\overline{x}_{aco,n}^{(i)} \leftarrow \widehat{x}_{aco,n}^{(i)}$, $\overline{x}_{aco,n+N/2}^{(i)} \leftarrow 0$,
  end if
  Calculate $\overline{X}_{aco,k}^{(i)}$ after N-point FFT,
  $\widetilde{X}_{aco,k}^{(i)} \leftarrow \mathrm{Re}\left(\frac{\overline{X}_{aco,k}^{(i)} + \overline{X}_{aco,N-k}^{(i)}}{2}\right) + j\mathrm{Im}\left(\frac{\overline{X}_{aco,k}^{(i)} - \overline{X}_{aco,N-k}^{(i)}}{2}\right)$,
  Calculate $\mathrm{BER}^{(i)}$,
  $i \leftarrow i + 1$,
until $i > T$ or $\mathrm{BER}^{(i-1)} < \tau$

Ensure:

Final estimations of ACO-OFDM and DCO-OFDM symbols: $\widetilde{X}_k^{(i)}$ and $\widetilde{Y}_k^{(i)}$.

TABLE 1. Simulation parameters.

Parameter	Explication	Value
N	The number of subcarriers	128
N_0	Noise PSD	2×10^{-9} A^2/Hz
I_H	Maximum allowed current	1
I_L	Minimum allowed current	0
M_A	Constellation order for ACO-OFDM	4
M_D	Constellation order for DCO-OFDM	4
T	The number of iterations	3
W	Bandwidth	100 MHz

low or high. That is because under this circumstance, with the increase of N_A, the average amplitudes A_P and A_N will decrease and increase, respectively.

The overall BER performance versus $\lambda\delta_A$ for $N_A = 64$ while β varies from 6 dB to 10 dB and $\eta_l = 13\%$ is shown in Fig. 6. In this case, the pure eADO-OFDM scheme is

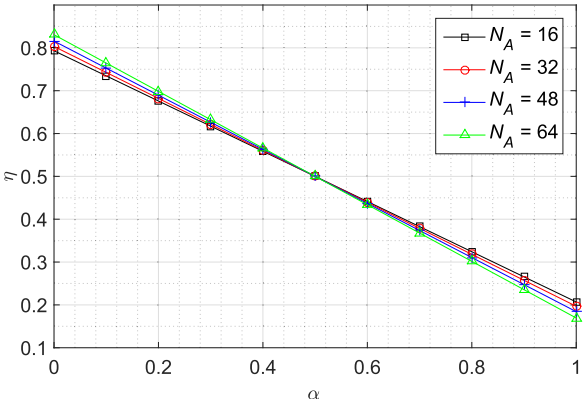

FIGURE 5. The dimming level η as a function of the ratio α with different N_A, while β is set as 10 dB.

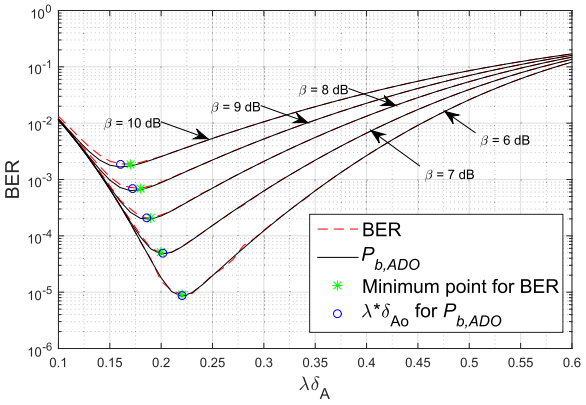

FIGURE 6. Overall BER performance versus $\lambda\delta_A$ with different β, while $N_A = 64$ and $\eta_l = 13\%$.

adopted due to the low dimming level. The black solid lines represent the BER calculated by (41) and the blue circles indicate $\lambda\delta_{Ao}$ calculated by (50), while the red dotted lines denote the actual BER obtained by simulation with their minimum points marked by green asterisks. It can be calculated according to (50) that for $\beta = 6$ dB, 7 dB, 8 dB, 9 dB, and 10 dB, $\lambda\delta_{Ao}$ are 0.22, 0.20, 0.19, 0.17, and 0.16, respectively, while optimal power allocations obtained by simulation are 0.22, 0.20, 0.19, 0.18, and 0.17, respectively. Thus, due to the mutual interference of ACO-OFDM and DCO-OFDM signals, the proposed power allocation scheme has the near-minimum overall BER. It can be seen that the overall BER performance of eADO-OFDM becomes better and worse when $\lambda\delta_A$ varies from 0.1 to $\lambda\delta_{Ao}$ and from $\lambda\delta_{Ao}$ to 0.6, respectively. That is because when $\lambda\delta_A$ is small, the BER of ACO-OFDM will be very high, resulting poor capability to regenerate the original ACO-OFDM, which will also impact the demodulation process of DCO-OFDM. Thus, with the increase of $\lambda\delta_A$, the overall BER performance will be better. However, when $\lambda\delta_A$ is greater than $\lambda\delta_{Ao}$, the BER of ACO-OFDM is already very small, and the BER of DCO-OFDM becomes the main factor determining the overall BER.

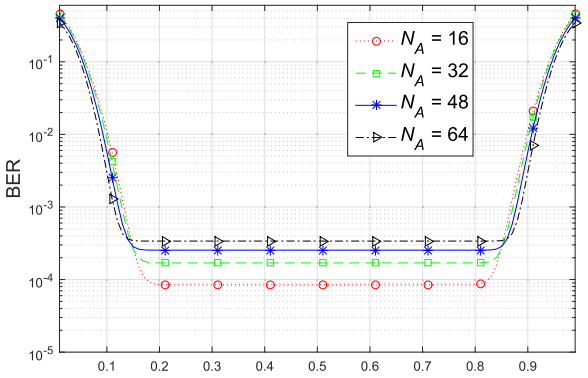

FIGURE 7. The BER performance as a function of η with different N_A, while $\beta = 8$ dB.

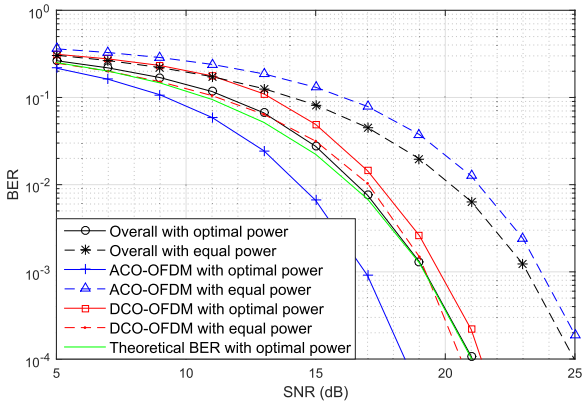

FIGURE 8. The BER performance with equal and proposed power allocations, while the conventional receiver is utilized and β, η_l, and N_A are set as 10 dB, 17%, and 64, respectively.

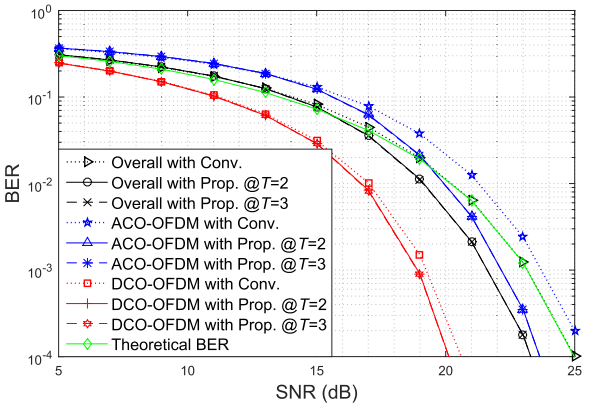

FIGURE 9. The BER performance comparison between the conventional and the proposed iterative receiver with equal power allocation, while β and N_A are set as 10 dB and 64, respectively.

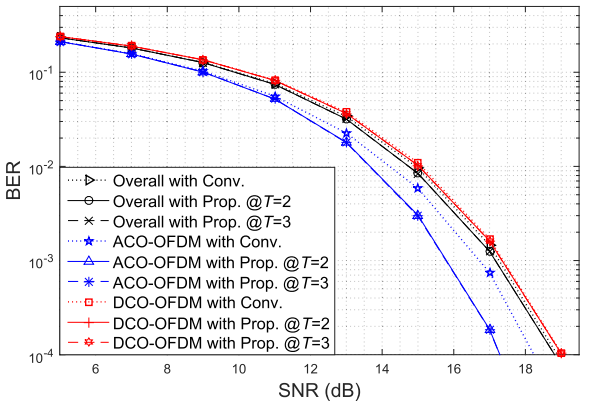

FIGURE 10. The BER performance comparison between the conventional and the proposed iterative receiver with optimal power allocation, while β and N_A are set as 7 dB and 32, respectively.

Fig. 7 shows the BER performance versus η with different N_A while $\beta = 8$ dB and fixed $\lambda\delta_A$ is assumed. For a fixed N_A, the graph can be divided into three sections with low, intermediate, and high dimming levels, respectively. For example, for $N_A = 16$, when the dimming level is between 0 and 21%, the pure eADO-OFDM is applied, and the BER reduces from 4×10^{-1} to 2.5×10^{-4}. That is because with the increase of η, $\lambda\delta_D$ will increase, resulting in the lower BER. When the dimming level is between 21% and 79%, the transmitted signal is a combination of eADO-OFDM and eNADO-OFDM signals, and the dimming control scheme is achieved by adjusting the ratio α, thus the BER will not change. When the dimming level is between 79% and 100%, the pure eNADO-OFDM is applied, and the BER increases from 2.5×10^{-4} to 4×10^{-1} because the decrease of $\lambda\delta_D$.

Fig. 8 shows the BER performance comparison between the equal and proposed power allocations with conventional receiver, while the bias-index β, the dimming level η_l, and the subcarrier number N_A for ACO-OFDM are set as 10 dB, 13%, and 64, respectively. It can be observed from Fig. 8 that the theoretical BER curve and the simulated overall BER curve match well, which means (41) can be a good theoretical result of the system's overall BER performance. The required SNR at an overall BER of 10^{-4} for the equal power allocation scheme is about 25 dB, while it decreases to 21 dB when the proposed power allocation scheme is adopted. Specifically, compared with the equal power allocation, the optical power allocated to ACO-OFDM is greatly increased in the proposed scheme. Correspondingly, the optical power allocated to the DCO-OFDM is reduced when optimal power allocation is performed. Thus, in this case, the proposed optimal power allocation technique will enhance the BER performance of ACO-OFDM, and the required SNR reduces from above 25 dB to 18.4 dB when the BER of ACO-OFDM signal is 10^{-4}. However, due to the worse effect of ACO-OFDM interference on the DCO-OFDM demodulation and the decreased optical power allocated to DCO-OFDM, the corresponding performance of DCO-OFDM will be degraded. But in this case, the ACO-OFDM performance improvement is dominant to DCO-OFDM performance degradation, in term of BER, thus, the overall BER performance is enhanced.

Fig. 9 shows the BER performance comparison between the conventional receiver ('Conv' for short) and the proposed iterative receiver ('Prop' for short) with equal power allocation, while β and N_A are set as 10 dB and 64, respectively.

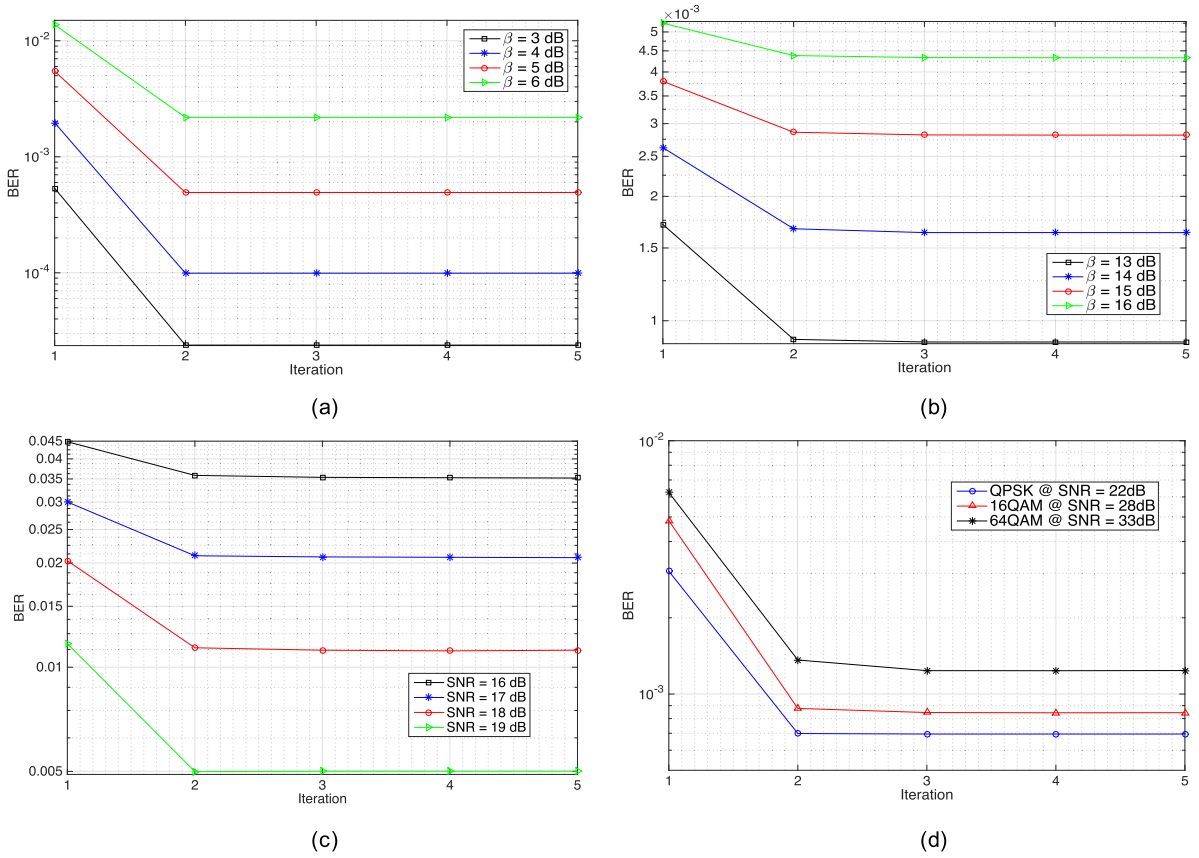

FIGURE 11. The convergence performance of the proposed iterative interference cancellation scheme. (a) Case 1: with low β, while the SNR and N_A are set as 22 dB and 64, respectively. (b) Case 2: with high β, while the SNR and N_A are set as 22 dB and 64, respectively. (c) Case 3: with low SNRs, while β and N_A are set as 10 dB and 64, respectively. (d) Case 4: with different modulation constellation schemes, while β and N_A are set as 10 dB and 64, respectively.

Like in Fig. 8, the theoretical BER curve and the simulated overall BER curve are well matched. It is evident that our proposed iterative receiver outperforms the conventional receiver. More specifically, at a BER of 10^{-4}, for ACO-OFDM, the proposed iterative receiver achieves more than 1.4 dB gains compared with the conventional receiver, for the reason that the pairwise averaging and pairwise clipping could mitigate the effect of noise and more accurate ACO-OFDM signal could be achieved. For DCO-OFDM, the proposed iterative receiver performs 0.5 dB gain than the conventional receiver because the interference introduced by the error estimation of ACO-OFDM signal will be reduced, so that the DCO-OFDM signal can be estimated more precisely. And for the overall BER performance, the iterative receiver performs 1.8 dB better than the conventional receiver with the improved ACO-OFDM and DCO-OFDM signals. Besides, it can be seen from the figure that the BER curves of $T = 2$ and $T = 3$ almost coincide, which means that the iterative interference cancellation scheme converges after only few iterations.

The BER performance comparison between the conventional and the proposed iterative receivers with optimal power allocation is shown in Fig. 10, while β and N_A are set as 7 dB and 32, respectively. At a BER of 10^{-4}, for ACO-OFDM, the proposed iterative receiver achieves about 1 dB gains compared to the conventional receiver. Because of the optimal power allocation, the BER of ACO-OFDM has been extremely small, thus the BER improvement of DCO-OFDM caused by iterative receiver is not significant in this scenario, resulting in little improvement of the overall BER performance. Similar to the equal power allocation scheme, the gap of the BER curves for $T = 2$ and $T = 3$ is also extremely small, which means that the iterative interference cancellation scheme with optimal power allocation also converges after only few iterations.

Fig. 11(a) and Fig. 11(b) are plotted to show the effect of bias-index β on the convergence of the iteration, while the SNR and N_A are set as 22 dB and 64, respectively. As seen in Fig. 11(a) and Fig. 11(b), even if the bias-index β is low or high, after only two or three iterations, the proposed iterative interference cancellation scheme will converge. Fig. 11(c) is intended to show the effect of SNRs on the convergence of the iteration, while β and N_A are set as 10 dB and 64, respectively. It can be seen that the proposed iterative interference cancellation scheme converges after only few iterations even if the SNR is low. Specifically, when the

SNR is below 19 dB, three iterations are required, while it converges after only 2 iterations when SNR = 19 dB. Generally, when the SNR is low, the number of required iterations is larger than that with a higher SNR. Fig. 11(d) is intended to shown the convergence performance of the proposed iterative interference cancellation scheme with different constellation orders, while β and N_A are set as 10 dB and 64, respectively. In order to maintain a BER of around 10^{-3}, different SNRs are carefully selected for different modulation orders. It can be seen from the figure that when the constellation order is high, the number of required iterations should be more.

VII. CONCLUSIONS

In this paper, the eADO-OFDM and eNADO-OFDM with subcarrier assignment are exploited to support various access conditions of services in downlink multiple access. To accommodate dimming requirements, a dimming control scheme is proposed where the eADO-OFDM and eNADO-OFDM signals are combined with a proper ratio. Then, the optimal power allocation is investigated to minimize the overall BER. Moreover, to mitigate the impact of noise and interference, an iterative interference cancellation scheme is proposed. Simulation results show that the proposed scheme can effectively achieve the dimming control scheme with a wide dimming range. In addition, compared with conventional scheme with equal power allocation, the proposed scheme with iterative interference cancellation and optimal power allocation can achieve superior BER performance at the same SNR, while only a few iterations are required to converge.

REFERENCES

[1] A. Jovicic, J. Li, and T. Richardson, "Visible light communication: Opportunities, challenges and the path to market," *IEEE Commun. Mag.*, vol. 51, no. 12, pp. 26–32, Dec. 2013.
[2] M. Z. Chowdhury, M. T. Hossan, A. Islam, and Y. M. Jang, "A comparative survey of optical wireless technologies: Architectures and applications," *IEEE Access*, vol. 6, pp. 9819–9840, 2018.
[3] Z. Wang, Q. Wang, S. Chen, and L. Hanzo, "An adaptive scaling and biasing scheme for OFDM-based visible light communication systems," *Opt. Express*, vol. 22, no. 10, pp. 12707–12715, May 2014.
[4] F. Yang, J. Gao, and S. Liu, "Novel visible light communication approach based on hybrid OOK and ACO-OFDM," *IEEE Photon. Technol. Lett.*, vol. 28, no. 14, pp. 1585–1588, Jul. 15, 2016.
[5] Y. Sun, F. Yang, and L. Cheng, "An overview of OFDM-based visible light communication systems from the perspective of energy efficiency versus spectral efficiency," *IEEE Access*, vol. 6, pp. 60824–60833, 2018.
[6] S. D. Dissanayake and J. Armstrong, "Comparison of ACO-OFDM, DCO-OFDM and ADO-OFDM in IM/DD systems," *J. Lightw. Technol.*, vol. 31, no. 7, pp. 1063–1072, Apr. 1, 2013.
[7] J. Armstrong and B. Schmidt, "Comparison of asymmetrically clipped optical OFDM and DC-biased optical OFDM in AWGN," *IEEE Commun. Lett.*, vol. 12, no. 5, pp. 343–345, May 2008.
[8] J. Armstrong and A. J. Lowery, "Power efficient optical OFDM," *Electron. Lett.*, vol. 42, no. 6, pp. 370–372, Mar. 2006.
[9] S. C. J. Lee, S. Randel, F. Breyer, and A. M. J. Koonen, "PAM-DMT for intensity-modulated and direct-detection optical communication systems," *IEEE Photon. Technol. Lett.*, vol. 21, no. 23, pp. 1749–1751, Dec. 1, 2009.
[10] S. D. Dissanayake, K. Panta, and J. Armstrong, "A novel technique to simultaneously transmit ACO-OFDM and DCO-OFDM in IM/DD systems," in *Proc. IEEE GLOBECOM Workshops (GC Wkshps)*, Dec. 2011, pp. 782–786.
[11] B. Ranjha and M. Kavehrad, "Hybrid asymmetrically clipped OFDM-based IM/DD optical wireless system," *IEEE/OSA J. Opt. Commun. Netw.*, vol. 6, no. 4, pp. 387–396, Apr. 2014.
[12] Q. Wang *et al.*, "Layered ACO-OFDM for intensity-modulated direct-detection optical wireless transmission," *Opt. Express*, vol. 23, no. 9, pp. 12382–12393, May 2015.
[13] J. Armstrong, "OFDM for optical communications," *J. Lightw. Technol.*, vol. 27, no. 3, pp. 189–204, Feb. 1, 2009.
[14] A. Weiss, A. Yeredor, and M. Shtaif, "Iterative symbol recovery for power-efficient DC-biased optical OFDM systems," *J. Lightw. Technol.*, vol. 34, no. 9, pp. 2331–2338, May 2016.
[15] F. Zafar, D. Karunatilake, and R. Parthiban, "Dimming schemes for visible light communication: The state of research," *IEEE Wireless Commun.*, vol. 22, no. 2, pp. 29–35, Apr. 2015.
[16] Z. Wang *et al.*, "Performance of dimming control scheme in visible light communication system," *Opt. Express*, vol. 20, no. 17, pp. 18861–18868, Aug. 2012.
[17] Y. Yang, Z. Zeng, J. Cheng, and C. Guo, "An enhanced DCO-OFDM scheme for dimming control in visible light communication systems," *IEEE Photon. J.*, vol. 8, no. 3, pp. 1–13, Jun. 2016.
[18] Q. Wang, Z. Wang, and L. Dai, "Asymmetrical hybrid optical OFDM for visible light communications with dimming control," *IEEE Photon. Technol. Lett.*, vol. 27, no. 9, pp. 974–977, May 1, 2015.
[19] F. Yang and J. Gao, "Dimming control scheme with high power and spectrum efficiency for visible light communications," *IEEE Photon. J.*, vol. 9, no. 1, Feb. 2017, Art. no. 7901612.
[20] L. Chen, B. Krongold, and J. Evans, "Performance analysis for optical OFDM transmission in short-range IM/DD systems," *J. Lightw. Technol.*, vol. 30, no. 7, pp. 974–983, Apr. 1, 2012.
[21] X. Li, J. Vucic, V. Jungnickel, and J. Armstrong, "On the capacity of intensity-modulated direct-detection systems and the information rate of ACO-OFDM for indoor optical wireless applications," *IEEE Trans. Commun.*, vol. 60, no. 3, pp. 799–809, Mar. 2012.
[22] Q. F. Lu, X. S. Ji, and K. Z. Huang, "Clipping distortion analysis and optimal power allocation for ACO-OFDM based visible light communication," in *Proc. 4th IEEE Int. Conf. Inf. Sci. Technol.*, Apr. 2014, pp. 320–323.
[23] X. Ling, J. Wang, X. Liang, Z. Ding, and C. Zhao, "Offset and power optimization for DCO-OFDM in visible light communication systems," *IEEE Trans. Signal Process.*, vol. 64, no. 2, pp. 349–363, Jan. 2016.
[24] R. Bai, R. Jiang, T. Mao, W. Lei, and Z. Wang, "Iterative receiver for ADO-OFDM with near-optimal optical power allocation," *Opt. Commun.*, vol. 387, pp. 350–356, Mar. 2017.
[25] J. Li, X.-D. Zhang, Q. Gao, Y. Luo, and D. Gu, "Exact BEP analysis for coherent M-ary PAM and QAM over AWGN and rayleigh fading channels," in *Proc. IEEE Veh. Technol. Conf. (VTC Spring)*, May 2008, pp. 390–394.
[26] K. Asadzadeh, A. Dabbo, and S. Hranilovic, "Receiver design for asymmetrically clipped optical OFDM," in *Proc. IEEE GLOBECOM Workshops (GC Wkshps)*, Dec. 2011, pp. 777–781.
[27] T. Wang, Y. Hou, and M. Ma, "A novel receiver design for HACO-OFDM by time-domain clipping noise elimination," *IEEE Commun. Lett.*, vol. 22, no. 9, pp. 1862–1865, Sep. 2018.

XUAN HUANG received the B.S. degree in electronic engineering from Tsinghua University, Beijing, China, in 2017, where she is currently pursuing the Ph.D. degree with the Department of Electronic Engineering. Her research interests include visible light communications, 5G wireless technologies, non-orthogonal multiple access, and signal processing techniques for communication systems.

FANG YANG (M'11–SM'13) received the B.S.E. and Ph.D. degrees in electronic engineering from Tsinghua University, Beijing, China, in 2005 and 2009, respectively, where he is currently an Associate Professor with the Department of Electronics Engineering. He has published over 120 peer-reviewed journal and conference papers. He holds over 40 Chinese patents and two PCT patents. His research interests include channel coding, channel estimation, interference cancellation, and signal processing techniques for communication systems, especially in power line communication, visible light communication, and digital television terrestrial broadcasting. He received the IEEE Scott Helt Memorial Award (Best Paper Award in IEEE TRANSACTIONS IN BROADCASTING), in 2015. He is the Secretary-General of the Sub-Committee 25 of the China National Information Technology Standardization (SAC/TC28/SC25). He currently serves as an Associate Editor for the IEEE ACCESS.

XUAN LIU received the M.S. degree from Tianjin University, Tianjin, China. He is currently the Deputy Chief Engineer with the Metering Department of the China Electric Power Research Institute. His research interest includes AMI systems.

HAILONG ZHANG received the M.S. degree from Tianjin University, Tianjin, China. He is currently an Engineer with the Metering Department, China Electric Power Research Institute. His research interests include power-line communication and wireless communication.

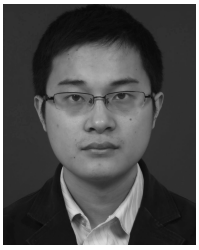

JUN YE received the M.S. degree from Chongqing University, Chongqing, China. He is currently an Engineer with the State Grid Chongqing Electric Power Company Electric Power Research Institute. His research interests include power-line communication and wireless communication.

JIAN SONG (M'06–SM'10–F'16) received the B.Eng. and Ph.D. degrees in electrical engineering from Tsinghua University, Beijing, China, in 1990 and 1995, respectively, and worked for the same university upon his graduation. He was with The Chinese University of Hong Kong, in 1996, and the University of Waterloo, Canada, in 1997. He has been with Hughes Network Systems, USA, for seven years before joining the faculty team in Tsinghua University, in 2005, as a Professor. He is currently the Director of Tsinghua's DTV Technology R&D Center. He has been involved in quite different areas of fiber-optic, satellite, and wireless communications, as well as the power-line communications. His current research interest includes digital TV broadcasting. He has published more than 200 peer-reviewed journal and conference papers. He holds two U.S. and more than 40 Chinese patents. He is Fellow of the IET.